Hindawi Publishing Corporation
Mathematical Problems in Engineering
Volume 2012, Article ID 597474, 13 pages
doi:10.1155/2012/597474

Research Article

Decomposition of the Time Reversal Operator for Target Detection

Chun-xiao Li,[1,2] Huan-cai Lu,[1,2] Ming-fei Guo,[1] Hang-fang Zhao,[3] and Jiang-ming Jin[1,2]

[1] *MOE Key Laboratory of Mechanical Manufacture and Automation, Zhejiang University of Technology, Hangzhou 310014, China*
[2] *Zhejiang Key Laboratory of Signal Processing, Zhejiang University of Technology, Hangzhou 310014, China*
[3] *Department of Information Science and Electronic Engineering, Zhejiang University, Hangzhou 310027, China*

Correspondence should be addressed to Chun-xiao Li, chunxiaoli@zju.edu.cn

Received 8 September 2012; Revised 6 November 2012; Accepted 12 November 2012

Academic Editor: Fatih Yaman

A thorough theory of detection problem using active time reversal has been investigated in several recent papers. Although active time reversal method is theoretically superior to the others, its practical implementation for target detection is far more difficult. This paper investigates the detection problem using passive decomposition of the time reversal operator (DORT) method. Provided that the signal components can be modeled as a linear combination of basis vectors with an unknown signal subspace, the generalized likelihood ratio test (GLRT) is derived based on Neyman-Person lemma with the unknown signal subspace replaced by its maximum likelihood estimation. The test statistics is one of the dominant eigenvalues of the time reversal operator for a point-like scatterer. Finally, the performance of the DORT detector is investigated with acoustic data collected from a waveguide tank. The experimental results show that the DORT detector can provide, respectively, 1.4 dB, 1.1 dB, and 0.8 dB performance gains over the energy detector given false alarms rate of 0.0001, 0.001, and 0.01.

1. Introduction

It is acoustically difficult to detect a target in shallow water environment, for instance, the performances of the traditional detectors such as the matched filter are severely degraded because the echo of active sonar undergoes distortion during two-way propagation and reflection from the target. One of the approaches to improve the detection performance is the model-based matched filter that takes advantage of the physical model to enhance signal

processing [1]. Another compromising solution is the one to model the channel distortion, such as the segmented replica correlation detector and the replica correlation integration detector [2, 3].

Time-reversal approaches provide an alternative approach to this kind of problem [4–7]. The unique feature of time reversal is that it provides a robust set of waves without any signal analysis, which compensates for the distortion induced by spatial inhomogeneities in the propagation medium [4]. Two time-reversal approaches, the iterative time-reversal, and the decomposition of the time reversal operator (DORT) can be employed for detection and localization of target [6–9].

Time reversal has been intensively studied in ultrasound acoustics and electromagnetics. There have been several recent studies devoted to the detection problem from the statistic signal processing perspective [10–15]. Reference [12] investigates the detection problem using the active time reversal of DORT method and the iterative time reversal method in the context of acoustic wave processing in ocean, while [10, 11] studies the active iterative time reversal method in the context of electromagnetic wave processing in air.

Although active time reversal method is theoretically superior to the others, its practical implementation for target detection is far more difficult. As an alternative, this paper investigates the detection problem using passive DORT method in acoustic wave processing in ocean. Compared to electromagnetic wave propagation in air, sound propagation in ocean is more environmentally involved. The terms "active" and "passive" refer to the source-receiver arrays (SRA): "active" array works when a SRA attempts to focus on a target by retransmitting an environmentally dependent excitation vector, while "passive" array functions when a SRA simply transmits signals from individual source elements followed by processing of the returned time series [16]. Moreover, the performances of the derived detectors in [12] are only evaluated by numerical simulations. This paper tests the detector with real acoustic data from waveguide experiments.

The rest of the paper is organized as follows. The mathematical model of binary hypothesis is derived, and the generalized likelihood ratio test (GLRT) of the DORT approach is developed in Section 2. The proposed detectors are validated by laboratory waveguide experiments in Section 3. The conclusions and summary are drawn in Section 4.

2. Theory and Method

2.1. Notations

We denote scalars by lowercase letters, vector quantities by boldface lowercase letters, and matrices by uppercase boldface. $(\cdot)^H$ stands for conjugate transpose; $R(A)$ and $I(A)$ are the real and the imaginary parts of matrix A, respectively; $\mathrm{tr}(\mathbf{A})$ is the sum of the diagonal elements of $\mathbf{A}$; $\mathbf{I}_N$ is the identity matrix of size N.

2.2. DORT Measurement

According to the theory of DORT, a SRA of N sensors collects data and then generates a response matrix with $N \times N$ dimension. The matrix is formed by sequentially transmitting signals from individual source elements of the SRA or orthogonal beams and recording the backscattered echo on each receiver element [8, 9, 17].

Provided that a normalized narrow-band signal is transmitted (the angular frequency ω is thus omitted in the formulas below), the received signals in time are first transformed into frequency domain. They can be modeled as a sum of interferences and possible signals whose presence we are trying to detect as follows:

$$\mathbf{y}_j = \mathbf{s}_j + \mathbf{v}_j, \quad j = 1, 2, \ldots, N, \tag{2.1}$$

where $\mathbf{s}_j$ is the signal term and $\mathbf{v}_j$ is the interference-plus-noise term for jth transmission.

The signal vector $\mathbf{s}_j$ is assumed to be deterministic but unknown. We model them as $\mathbf{s}_j = \mathbf{H}\boldsymbol{\theta}_j$, which are a linear combination of basis vectors with an unknown signal subspace $\mathbf{H}$ with known rank-p (corresponding to p propagation modes of a scatterer). Considering that the target is not definitely a point-like scatterer for the application of DORT method, the signal subspace has dimension p. In practical implementation, $\mathbf{H}$ is a $N \times p$ matrix, and each column $\mathbf{h}_i$ is the Green's function of the channel between the SRA and one aspect of the scatterer.

Although the interference $\mathbf{v}_j$ is the sum of the receiver noise and the reverberation signal, the DORT method has the ability to separate the echo of a target from reverberation [18]. We assume that both the receiver noise and the residual reverberation signal can be modeled as zero-mean white Gaussian random processes [2], that is,

$$\mathbf{v}_j \sim CN\left(0, \sigma_v^2 \mathbf{I}_N\right). \tag{2.2}$$

The real and imaginary components of $\mathbf{v}_j$ are $R(\mathbf{v}_j) \sim N(0, (\sigma_v^2/2)\mathbf{I}_N)$ and $I(\mathbf{v}_j) \sim N(0, (\sigma_v^2/2)\mathbf{I}_N)$, respectively. Although the assumption of Gaussian reverberation may not always be true, it is often made to facilitate mathematical analysis.

After all the transmission are finished, the total received data can be arranged as a matrix by [19]

$$\mathbf{Y} = \left[\mathbf{y}_1 \vdots \cdots \vdots \mathbf{y}_j \vdots \cdots \vdots \mathbf{y}_N\right]. \tag{2.3}$$

Similarly, the signal matrix can be written as $\mathbf{S} = [\mathbf{s}_1 \vdots \cdots \vdots \mathbf{s}_j \vdots \cdots \vdots \mathbf{s}_N]$.

The detection problem then becomes to choose one of the following two hypotheses:

$$H_0 : \mathbf{Y} = \mathbf{V} \qquad \text{versus} \qquad H_1 : \mathbf{Y} = \mathbf{S} + \mathbf{V}. \tag{2.4}$$

2.3. *The DORT Detector*

As shown in [10, 12], the suboptimal detector using GLRT in the Neyman-Pearson sense is derived as an energy detector in conventional approaches when the Green's function of unknown channel is replaced by its maximum likelihood estimation. In this paper a suboptimal detector using the GLRT approach is derived for the time reversal approach, which is named the DORT detector.

The probability density functions (PDF) $p(\mathbf{Y} \mid H_1)$ and $p(\mathbf{Y} \mid H_0)$ under condition of H_1 and H_0 are, respectively,

$$p(\mathbf{Y} \mid H_1) = \frac{1}{\pi^{NN}\left(\sigma_v^2\right)^{NN}} e^{\mathrm{tr}(-[(\mathbf{Y}-\mathbf{S})(\mathbf{Y}-\mathbf{S})^H]/\sigma_v^2)},$$
$$p(\mathbf{Y} \mid H_0) = \frac{1}{\pi^{NN}\left(\sigma_v^2\right)^{NN}} e^{\mathrm{tr}(-[\mathbf{Y}\mathbf{Y}^H]/\sigma_v^2)}. \tag{2.5}$$

Recall that the generalized likelihood ratio is defined by the ratio of the likelihood functions under each hypothesis, but it is maximized over the unknown nuisance parameter space [20], that is,

$$\max_{\Theta} \frac{p(\mathbf{Y} \mid H_1, \Theta)}{p(\mathbf{Y} \mid H_0)}, \tag{2.6}$$

where Θ denotes the nuisance parameter set, for example, the unknown signal subspace $\mathbf{H}$.

It is assumed that the statistical characterization of the noise is completely known a priori in this paper. Then the detection problem becomes finding a maximum likelihood estimate of the signal subspace $\mathbf{H}$, or equivalently, its orthogonal subspace $\mathbf{A} = [\mathbf{a}_{p+1} \cdots \mathbf{a}_N]$ under condition of H_1 [21]. The log-likelihood function of $\mathbf{Y}$ under H_1 is (ignoring constants)

$$L = \ln p(\mathbf{Y} \mid H_1) = -\frac{1}{\sigma_v^2} \mathrm{tr}\Big[(\mathbf{Y} - \mathbf{S})^H (\mathbf{Y} - \mathbf{S})\Big]. \tag{2.7}$$

A maximum likelihood principle to identify the orthogonal subspace $\mathbf{A}$ can form a Lagrangian for minimizing $-2\sigma_v^2 L$ in (2.7) under the constraints $\mathbf{a}_i^H \mathbf{S} = [0 \cdots 0]$:

$$\ell = \mathrm{tr}\Big[(\mathbf{Y} - \mathbf{S})^H (\mathbf{Y} - \mathbf{S})\Big] + 2\,\mathrm{tr}\Big(\mathbf{A}^H \mathbf{S} \Xi\Big), \tag{2.8}$$

where Ξ is an $(N - p) \times N$ matrix, it contains the Lagrangians ξ_{ij}.

Firstly, we can estimate the signal matrix $\mathbf{S}$ assuming that the orthogonal subspace $\mathbf{A}$ is known, and then we further maximize likelihood with respect to $\mathbf{A}$ (cf. [21] for detailed derivations). The estimate of signal matrix is

$$\widehat{\mathbf{S}} = (\mathbf{I} - P_{\mathbf{A}})\mathbf{Y}, \tag{2.9}$$

where $P_{\mathbf{A}}$ is the projection $P_{\mathbf{A}} = \mathbf{A}(\mathbf{A}^H \mathbf{A})^{-1} \mathbf{A}^H$.

Substitute (2.9) into (2.7), we obtain

$$L = -\frac{1}{\sigma_v^2} \mathrm{tr}\Big[P_{\mathbf{A}} \mathbf{Y}\mathbf{Y}^H\Big]. \tag{2.10}$$

In practice, $\mathbf{Y}$ is the measurement of the transfer matrix, and $\mathbf{R} = \mathbf{Y}\mathbf{Y}^H$ is the time reversal operator. As the subspace $\mathbf{A}$ is unknown, we must further maximize likelihood with respect to it.

Let the time reversal operator have the orthogonal decomposition below

$$\begin{aligned} \mathbf{R} &= \mathbf{U}\Lambda^2\mathbf{U}^T, \\ \mathbf{U} &= \left[\mathbf{u}_1 \cdots \mathbf{u}_{p+1} \cdots \mathbf{u}_N\right], \\ \Lambda^2 &= \operatorname{diag}\left\{\lambda_1^2 \cdots \lambda_{p+1}^2 \cdots \lambda_N^2\right\}, \end{aligned} \tag{2.11}$$

where the eigenvalue matrix Λ^2 is sorted in descending order, and the matrix $\mathbf{U}$ is composed of the corresponding eigenvectors. It is then straightforward proved that L is bounded as follows:

$$L \le -\frac{1}{\sigma_v^2}\sum_{i=p+1}^{N}\lambda_i^2 \tag{2.12}$$

for any rank-$N-p$ projector $P_{\mathbf{A}}$.

If $\widehat{\mathbf{A}} = [\mathbf{u}_{p+1} \cdots \mathbf{u}_N]$, the bound is achieved for a projector $P_{\mathbf{A}}$ onto the subspace $\langle\widehat{\mathbf{A}}\rangle$:

$$P_{\mathbf{A}} = \widehat{\mathbf{A}}\widehat{\mathbf{A}}^H. \tag{2.13}$$

Clearly, the dominant p eigenvectors form a rank-p signal subspace, and the rest of the eigenvectors builds a rank-$N-p$ orthogonal subspace $\mathbf{A}$. The estimate of the signal subspace is

$$\widehat{\mathbf{H}} = \left[\mathbf{u}_1 \cdots \mathbf{u}_p\right]. \tag{2.14}$$

Substituting (2.5), (2.9), and (2.13) into (2.6), and taking the logarithm operation with constants neglected yields

$$\begin{aligned} L_{\mathrm{DORT}} &= -\frac{1}{\sigma_v^2}\operatorname{tr}\left[(\mathbf{Y}-\mathbf{S})^H(\mathbf{Y}-\mathbf{S})\right] + \frac{1}{\sigma_v^2}\operatorname{tr}\left[\mathbf{Y}^H\mathbf{Y}\right] \\ &= -\frac{1}{\sigma_v^2}\sum_{i=p+1}^{N}\lambda_i^2 + \frac{1}{\sigma_v^2}\sum_{i=1}^{N}\lambda_i^2 = \frac{1}{\sigma_v^2}\sum_{i=1}^{p}\lambda_i^2. \end{aligned} \tag{2.15}$$

Recall that only a single target is considered, that is, $p = 1$. That means

$$L_{\mathrm{DORT}} = \frac{1}{\sigma_v^2}\lambda_1^2. \tag{2.16}$$

Therefore the test statistic is one of the dominant eigenvalues of the time reversal operator if the signal components are assumed deterministic unknown and modeled as

a linear combination of basis vectors with an unknown signal subspace. The test statistic with minimal signal analysis is similar as that obtained in [19], which is $1 + \lambda_1^2$. We call it DORT detector. Due to its simple procedure of signal processing and no knowledge about the environment and the array configuration required, the DORT detector can be used to coarsely search the suspicious objects as a preliminary detector. In next section, we compare the detection performance of DORT detector with energy detector that is based on the same detection theory.

3. Experimental Results of Detector Performance

Since it is difficult to theoretically analyze the receiver-operating characteristics (ROC) of the DORT detector, we study the ROC by Monte Carlo simulation. This section presents the study on the detection performance of the DORT detector and the performance gain of DORT detector over the energy detector with a mix of real acoustic data from waveguide experiments and simulated noise.

3.1. Experimental Setup

The experimental setup is shown in Figure 1. The experiment was performed in a waveguide tank using a vertical SRA of 32 elements equally spaced at 0.04 m apart. The waver tank can simulate a stationary shallow water environment with multipath propagations, mainly including direct path, sea surface-reflected path, and sea bottom-reflected path. Each of the 32 elements is individually controlled and amplified during transmission and reception. The waveguide tank is 14 m in length, 1.2 m in width, and 1.4 m in height. Its three of four vertical walls are covered with anechoic tiles, the other one is a steel sheet located 12 m away from the SRA. The bottom is a sandstone basement covered with sand of 0.22 m thickness.

The transmitted signal is a 0.5 ms PCW signal centered at 18 kHz. The wavelength is about 0.08 m. The first source transducer is excited by the transmitted signal. The backscattered waves received on the N channels of the SRA are stored. This operation is repeated for all the transducers. Finally a data matrix $\mathbf{Y}$ is generated. The target was an air-filled steel cylinder of 0.21 m ($2.6\,\lambda$) in diameter and 0.51 m ($6.2\,\lambda$) in length suspended at a range of 8.2 m and a depth of 0.84 m. This means that the range of target to SRA is about $100\,\lambda$ and suspended at depth of $10.5\,\lambda$.

The water column has a sound of equal speed profile. The bottom is modeled as a 0.22 m sand sediment layer above a sandstone basement. The environmental parameters are following: in the water column, wave speed $c_1 = 1480\,\text{m/s}$; in the bottom layer, sand density $\rho_2 = 1800\,\text{kg/m}^3$, sand speed $c_2 = 1650\,\text{m/s}$, and attenuation $\alpha_2 = 0.67\,\text{dB}$ per wavelength; in the basement layer, density $\rho_3 = 1800\,\text{kg/m}^3$, speed $c_3 = 1580\,\text{m/s}$, and attenuation $\alpha_3 = 0.8\,\text{dB}$ per wavelength.

3.2. Signal Processing

In order to obtain high SNR, the time reversal operator is built from short time windows. That is, the matrix $\mathbf{Y}(\omega, r)$ is the Fourier transform $\mathbf{Y}(t)$ (the measurement of transfer matrix $\mathbf{K}(t)$ between time t and $t + \Delta t$, where t is related to the distance r through the equation $t = 2r/c$; c is the sound speed; Δt is the window length [18]. Especially, r_0 corresponds to the distance

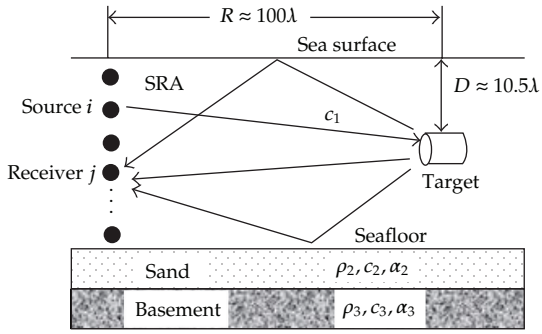

Figure 1: Experimental setup and model for the acoustic environment.

of the target. In order to obtain the test statistic in (2.16) using DORT observation matrix $\mathbf{Y}^H\mathbf{Y}$, the range of the target is firstly estimated. The matrix containing the target echo is then transformed into frequency domain. Finally the test statistic is got by the SVD decomposition of the matrix. A detailed illustration is shown in this section.

To estimate the distance of the target, a $\Delta t = 0.5$ ms time windows is shifted by steps of 0.25 ms. The selection of the windows length will be illustrated later on. For each distance$r$, the matrices $\mathbf{Y}(r)$ are calculated at center frequency 18 kHz. After SVD decomposition, the first eigenvalues are normalized. In the approach of the energy detector, the average energy of the array at center frequency for each transmission is firstly calculated and then is accumulated to obtain the total average energy for the all transmissions. There is another simple method to calculate the energy is to summarize all eigenvalues after SVD decomposition.

Figure 2 depicts the first normalized eigenvalues and the normalized energies as a function of distance from 0 to 20 m. It can be seen that a peak value appears, respectively, at the distance of 8.3 m for DORT detector and 8.4 m for the energy detector, which tells that both detectors can correctly detect the target (the other peak at the distance of 12 m is caused by the steel sheet).

It is worth noting that the target cannot be simply treated as a point-like scatterer compared to the wavelength. It has been shown that the diagonalization of the time-reversal operator permits the various elastic components of the scattered field to be extracted, and more than one eigenvalue is associated to the scatterer [7]. However, it has been also shown the strong specular echo can be separated from the Lamb wave by selecting temporally with a proper time window in the same reference.

Since the distance of the target has been determined, the corresponding time window $\mathbf{Y}(\omega, r_0)$ which contains the target echo can also be determined. This time-windowed segment of echo data is used for the following signal analysis and detection performance investigation. Figure 3 shows eigenvalues of the time-reversal operator at the central frequency for the windows of increasing duration of $\Delta t = 0.5$, 1, 1.5, and 2 ms. With the window duration increasing, all eigenvalues except the first one which is normalized are becoming larger and larger. It is possible that other propagation modes from the target or reverberation from other objects contribute to the signals in the time windows for long durations. Hence by choosing $\Delta t = 0.5$ ms as the window duration and selecting the time window associated to the strong specular echo, we still use the first eigenvalue as the test statistic for the DORT detector.

The backpropagation of the first eigenvector is calculated for the center frequency using KRAKEN [22]. The code KRAKEN is a normal mode propagation model developed

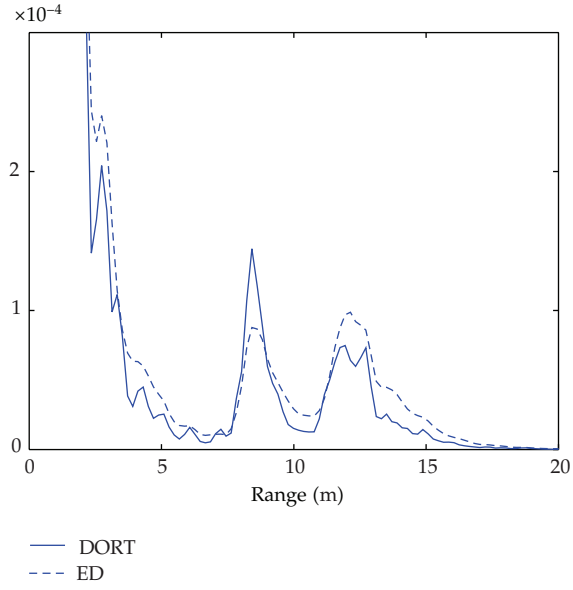

Figure 2: Target at 8.2 m: the first normalized eigenvalues (solid line) and the normalized energies (dashed line) as a function of distance from 0 m to 20 m.

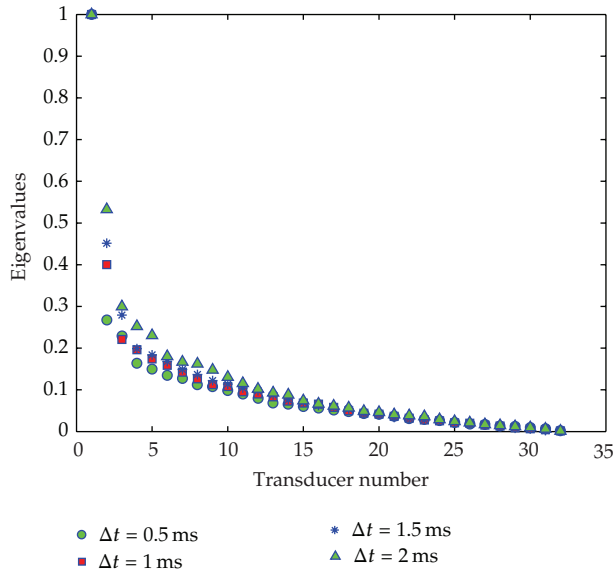

Figure 3: The experimental eigenvalues of of the time-reversal operator at the central frequency and the window duration is $\Delta t = 0.5$ ms(circle), $\Delta t = 1$ ms (square), $\Delta t = 1.5$ ms (star), and $\Delta t = 2$ ms (triangle).

at SACLANT Undersea Research Centre (now Nato Undersea Research Centre). It has been widely used for modeling ocean environments that are range independent, range dependent, or fully 3-dimensional. The image is displayed in the range from 1 m to 12 m on the whole height of the waveguide. As shown in Figure 4, the peak position in the ambiguity surface is at a range of 8.47 m and a depth of 0.85 m. The image provides information about the location

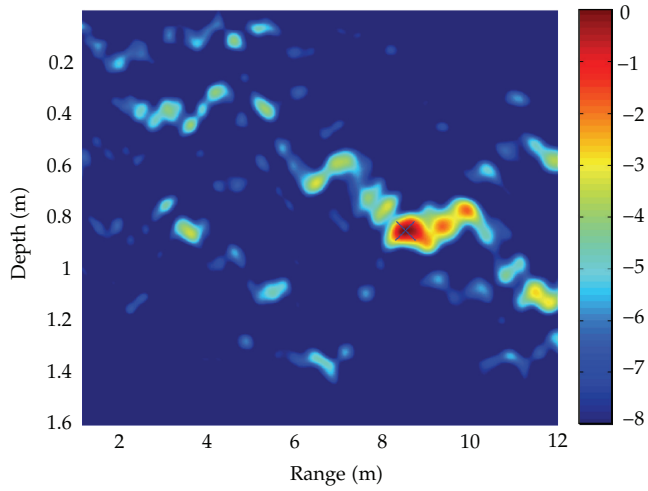

Figure 4: Numerical backpropagation of the first eigenvector using KRAKEN.

of the target, in almost agreement with the true position (8.2 m in range and 0.84 m in depth). The slight discrepancy is possibly caused by inexact environmental parameters in Figure 1.

3.3. Detection Performance

As mentioned in [23, 24], no analytical expression is available for the probability distribution of the first eigenvalue. Therefore, it is difficult to analytically express detection probability of DORT detector. The detection performance of DORT detector is numerically evaluated using Monte Carlo method.

The initial SNR is calculated by the ratio of the signal energy of the target cell to the energy of the time window near the target cell, which is about 8.2 dB. Note that the initial SNR is high, we considered that the corresponding time window $\mathbf{Y}(\omega, r_0)$ only contains the target echo; that is, the signal matrix is replaced by $\mathbf{Y}(\omega, r_0)$ containing noise in practice. To obtain noisy backscatter at different SNR, we added numerically generated zero-mean white Gaussian noise to the real data of acoustic backscatter [10]. The SNR is defined as

$$\text{SNR} = \frac{E\left\{\|\mathbf{S}\|^2\right\}}{E\left\{\|\mathbf{V}\|^2\right\}} = \frac{\sum_{j=1}^{N}\|\mathbf{s}_j\|^2}{N\sigma_v^2}. \tag{3.1}$$

For the practical signal processing, we set $\boldsymbol{\sigma}_{\mathbf{v}} = 1$ and scale the total signal energy to meet different SNR level. We then further modified the SNR levels in (3.1) according to the initial SNR to obtain values close to the actual ones.

To study the performance, we evaluated the detection probability P_D as a function of the SNR for a fixed probability of false alarm P_{FA}. In order to obtain the detection threshold, we, respectively, generated 10000 independent noise realizations and computed the test statistics given by (2.16) for DORT detector; the resulting 10000 test statistics are, respectively, sorted in ascending order; the thresholds are then selected so that $P_{\text{FA}} = 0.0001$, $P_{\text{FA}} = 0.001$, or $P_{\text{FA}} = 0.01$. To compute P_D, a new set of 5000 independent noise is generated and added

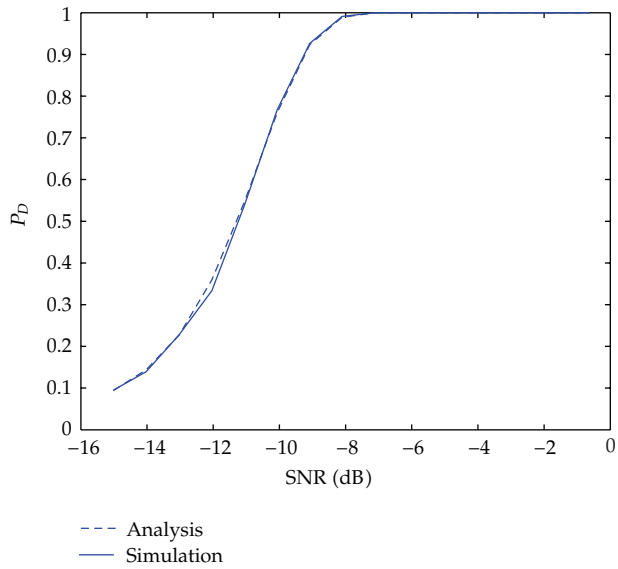

Figure 5: Detection probability versus SNR for $P_{FA} = 0.01$ using the energy detector with a mix of real acoustic data from laboratory waveguide experiment and simulated noise; analysis (dashed line) versus simulation (solid line).

to the actual acoustic data. The test statistics are, respectively, computed and compared to the corresponding thresholds. The percentage of the number of times that the test statistic exceeds the threshold is used as an estimate of the detection probability.

Figure 5 shows the results of simulation versus the ones of the energy detector for $P_{FA} = 0.01$ developed in [12]. Figure 5 indicates that the simulation result of the energy detector is in excellent agreement with the theoretical analysis, thus it validated the proposed design of simulation experiment with a mix of real acoustic data from laboratory waveguide experiment and simulated noise. Figure 6 shows the detection performance of DORT detector and that of the energy detector. It can be seen that DORT detector provides detection gain with respect to the energy detector, except that the energy detector performs better in the case that the detection probabilities for both detectors is lower than 0.2 for extremely low SNR. For instance, we measured the performance gains by the relative SNR required to achieve detection probabilities of 0.5 given false alarm rates of 0.0001, 0.001, and 0.01. The performance gains of the DORT detector with respect to the energy detector are respectively about, 1.4 dB, 1.1 dB, and 0.8 dB. It should be pointed out that no knowledge and modeling of the propagation medium are needed for the design of DORT detector.

The reason that the DORT detector has performance gain over energy detector can be explained as follows. In fact, the test statistic of the energy detector can also be expressed as the summarization of all eigenvalues $\lambda_1^2 + \lambda_2^2 + \cdots \lambda_N^2$ after SVD decomposition, instead of λ_1^2 for the DORT detector. The increment of the first eigenvalue is relatively larger than that of the others with SNR increasing, which can be implied in Figure 3. With the window duration increasing, the others are being more and more small compared to the first eigenvalue due to more noises are contained in the observation matrix.

4. Conclusion

In this paper, the target detection using passive DORT method is presented and discussed. The mathematical models of detection problem are developed using a sequence of collected

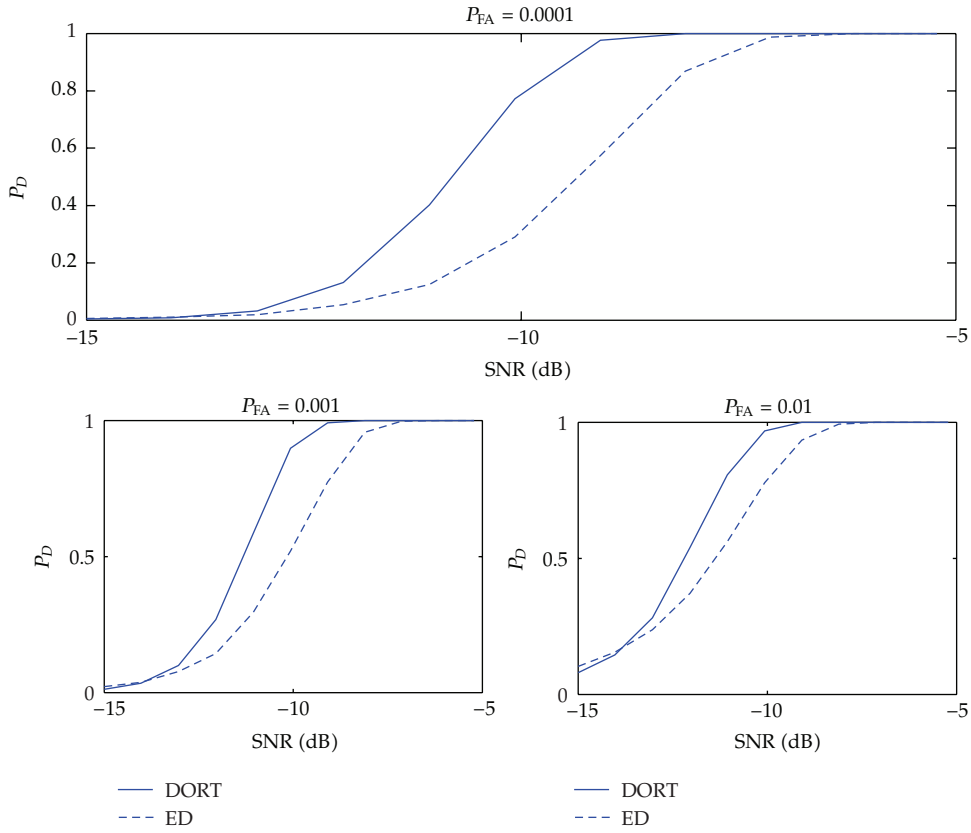

Figure 6: Detection probability versus SNR using a mix of real acoustic data from laboratory waveguide experiment and simulated noise; DORT detector (solid line) versus energy detector (dashed line).

data from typical DORT transmission. It is proved that the DORT detector can be derived with the unknown signal subspace replaced by its maximum likelihood estimate, if the signal components are assumed deterministic unknown and modeled as a linear combination of basis vectors with an unknown signal subspace; in addition, one of the dominant eigenvalue of the time reversal operator is the test statistic for point-like scatterer. Finally, the DORT detector and the energy detector are tested with the real acoustic data collected in the laboratory waveguide experiment.

The detection experiments using DORT method are conducted with the data measured from a 32 elements vertical SRA. A target has been detected and correctly located within the water depth. The experimental results show that the DORT detector can provide, respectively, 1.4 dB, 1.1 dB, and 0.8 dB performance gains over the energy detector given false alarms rate of 0.0001, 0.001, and 0.01. It should be pointed out that this paper only focuses on the passive time reversal method in which the SRA simply transmits conventional signals followed by processing of the returned time data series. Therefore, the detection gain is mainly provided by the decomposition that can separate the target echo from other contributions, but not by the adaption, say, the transmitted wavefront matched to the channel as the active time reversal methods. For future work, the detection problems for p independent point-like scatterers or in unstationary ocean environments using DORT method should be further investigated.

Acknowledgments

The authors gratefully acknowledge the support for the waveguide experiment from Hangzhou Applied Acoustics Research Institute. This work was supported by the Natural Science Foundation of China (Project no. 61101231), the Zhejiang Provincial Natural Science Foundation of China (Project no. Y1100629 and Y1100883), and the Foundation of Qianjiang Scholars (Project no. 56710203012).

References

[1] J. P. Hermand and W. I. Roderick, "Acoustic model-based matched filter processing for fading time-dispersive ocean channels: theory and experiment," *IEEE Journal of Oceanic Engineering*, vol. 18, no. 4, pp. 447–465, 1993.

[2] B. Friedlander and A. Zeira, "Detection of broadband signals in frequency and time dispersive channels," *IEEE Transactions on Signal Processing*, vol. 44, no. 7, pp. 1613–1622, 1996.

[3] P. M. Baggenstoss, "On detecting linear frequency-modulated waveforms in frequency- and time-dispersive channels: alternatives to segmented replica correlation," *IEEE Journal of Oceanic Engineering*, vol. 19, no. 4, pp. 591–598, 1994.

[4] P. Roux and M. Fink, "Time reversal in a waveguide: study of the temporal and spatial focusing," *Journal of the Acoustical Society of America*, vol. 107, no. 5, pp. 2418–2429, 2000.

[5] C. Prada, F. Wu, and M. Fink, "The iterative time reversal mirror: a solution to self-focusing in the pulse echo mode," *Journal of the Acoustical Society of America*, vol. 90, no. 2, pp. 1119–1129, 1991.

[6] N. Mordant, C. Prada, and M. Fink, "Highly resolved detection and selective focusing in a waveguide using the D.O.R.T. method," *Journal of the Acoustical Society of America*, vol. 105, no. 5, pp. 2634–2642, 1999.

[7] C. Prada and M. Fink, "Separation of interfering acoustic scattered signals using the invariants of the time—reversal operator: application to Lamb waves characterization," *Journal of the Acoustical Society of America*, vol. 104, no. 2, pp. 801–807, 1998.

[8] C. Prada, J. L. Thomas, and M. Fink, "The iterative time reversal process: analysis of the convergence," *Journal of the Acoustical Society of America*, vol. 97, no. 1, pp. 62–71, 1995.

[9] J. L. Li, H. F. Zhao, and W. Fang, "Experimental investigation of selective localisation by decomposition of the time reversal operator and subspace-based technique," *IET Radar, Sonar and Navigation*, vol. 2, no. 6, pp. 426–434, 2008.

[10] J. M. F. Moura and Y. Jin, "Detection by time reversal: single antenna," *IEEE Transactions on Signal Processing*, vol. 55, no. 1, pp. 187–201, 2007.

[11] Y. Jin and J. M. F. Moura, "Time-reversal detection using antenna arrays," *IEEE Transactions on Signal Processing*, vol. 57, no. 4, pp. 1396–1414, 2009.

[12] C. X. Li, W. Xu, J. L. Li, and X. Y. Gong, "Time-reversal detection of multidimensional signals in underwater acoustics," *IEEE Journal of Oceanic Engineering*, vol. 36, no. 1, pp. 60–70, 2011.

[13] S. Y. Chen, H. Tong, and C. Cattani, "Markov models for image labeling," *Mathematical Problems in Engineering*, vol. 2012, Article ID 814356, 18 pages, 2012.

[14] C. Cattani, S. Chen, and G. Aldashev, "Information and modeling in complexity," *Mathematical Problems in Engineering*, vol. 2012, Article ID 868413, 4 pages, 2012.

[15] S. Y. Chen, "Kalman filter for robot vision: a survey," *IEEE Transactions on Industrial Electronics*, vol. 59, no. 11, pp. 4409–4420, 2012.

[16] H. C. Song, W. S. Hodgkiss, W. A. Kuperman, K. G. Sabra, T. Akal, and M. Stevenson, "Passive reverberation nulling for target enhancement," *Journal of the Acoustical Society of America*, vol. 122, no. 6, pp. 3296–3303, 2007.

[17] J. F. Lingevitch, H. C. Song, and W. A. Kuperman, "Time reversed reverberation focusing in a waveguide," *Journal of the Acoustical Society of America*, vol. 111, no. 6, pp. 2609–2614, 2002.

[18] C. Prada, J. De Rosny, D. Clorennec et al., "Experimental detection and focusing in shallow water by decomposition of the time reversal operator," *Journal of the Acoustical Society of America*, vol. 122, no. 2, pp. 761–768, 2007.

[19] S. Bose and A. O. Steinhardt, "Adaptive array detection of uncertain rank one waveforms," *IEEE Transactions on Signal Processing*, vol. 44, no. 11, pp. 2801–2809, 1996.

[20] S. M. Kay, *Fundamentals of Statistical Signal Processing, Detection Theory*, Prentice Hall, PTR Press, Upper Saddle River, NJ, USA, 1998.
[21] L. L. Scharf, *Statistical Signal Processing: Detection, Estimation, and Time Series Analysis*, Addison-Wesley Press, New York, NY, USA, 1991.
[22] M. B. Porter, "The KRAKEN normal mode program," Memorandum SM-245, 1991.
[23] A. Aubry and A. Derode, "Detection and imaging in a random medium: a matrix method to overcome multiple scattering and aberration," *Journal of Applied Physics*, vol. 106, no. 4, Article ID 044903, 2009.
[24] A. Aubry and A. Derode, "Singular value distribution of the propagation matrix in random scattering media," *Waves in Random and Complex Media*, vol. 20, pp. 333–363, 2010.